Independence of fragment charge distributions of the size of heavy multifragmenting sources

M F. Rivet, C O. Bacri, B. Borderie, J.D. Frankland, M. Assenard, G. Auger, F. Bocage, R. Bougault, R. Brou, P. Buchet, et al.

[redacted]

Comparison between data measured by INDRA and the prediction of the BNV transport model for $^{36}Ar + ^{58}Ni$ reaction at 95 A.MeV

E. Galichet[4], F. Gulminelli[2], D.C.R. Guinet[4],
M. Assenard[6], G. Auger[3], Ch-O. Bacri[1], F. Bocage[2], B. Borderie[1],
R. Bougault[2], R. Brou[2], P. Buchet[5], J-L. Charvet[5], A. Chbihi[3], J. Colin[2],
D. Cussol[2], R. Dayras[5], A. Demeyer[4], D. Doré[5], D. Durand[2], P. Eudes[6],
J.D. Frankland[1], E. Genouin-Duhamel[2], E. Gerlic[4], M. Germain[6],
D. Gourio[6], P. Lautesse[4], J-L. Laville[6], J-F. Lecolley[2], A. Le Fèvre[3],
T. Lefort[2], R. Legrain[5], N. LeNeindre[2], O. Lopez[2], M. Louvel[2],
A-M. Maskay[6], L. Nalpas[5], A.D. Nguyen[2], M. Parlog[7], J. Péter[2],
E. Plagnol[1], G. Politi[9], A. Rahmani[6], T. Reposeur[6],M-F.Rivet[1],
E. Rosato[8], F. Saint-Laurent[3], S. Salou[3], J-C. Steckmeyer[2],
M. Stern[4], G. Tabacaru[7], B. Tamain[2], L. Tassan-Got[1], O. Tirel[3],
E. Vient[2], C. Volant[5] and J-P. Wieleczko[3].

[1]IPN Orsay, IN2P3-CNRS, 91406 Orsay Cedex, France.
[2]LPC, IN2P3-CNRS et Université, 14050 Caen Cedex, France.
[3]GANIL, CEA et IN2P3-CNRS, B.P. 5027, 14021 Caen Cedex, France.
[4]IPN Lyon, IN2P3-CNRS et Université, 69622 Villeurbanne, Cedex, France.
[5]DAPNIA/SPhN, CEA/Saclay, 91191 Gif-sur-Yvette Cedex, France.
[6]SUBATECH, IN2P3-CNRS et Université, 44072 Nantes Cedex 03, France.
[7]Nuclear Inst. for Physics and Nuclear Engineering, Bucharest, Roumania.
[8]INFN and Dip. di Fisica, Univ. di Napoli, 80125 Napoli, Italia.
[9]INFN and Dip. di Fisica, Univ. di Catania, 95129 Catania, Italia.

19th March 1998

Abstract

The reaction mechanisms and dynamical properties of the $^{36}Ar + ^{58}Ni$ system at 95 A.MeV measured by INDRA are studied within the BNV kinetic equation. A general protocol of comparison between the N-body experimental fragment information and the one-body distribution function is developed by means of an

intensive use of global variables.
We shall discuss the feasibility of such an approach and the distorsions induced by the finite detection efficiency and the completeness requirements of data selection. We shall study in some details the sensitivity of the different global observables to the macroscopic parameters of the effective nuclear interaction. In particular, the N/Z equilibration and neutron richness of the intermediate rapidity region will be adressed and some consequences on the symmetry energy of the nuclear mean field will be drawn.

1 Introduction

The study of reaction mechanisms in heavy ion collisions has much advanced recently with the construction of 4π detectors, like INDRA, which have high geometrical efficiency, good granularity and low detection energy thresholds. Thanks to these detectors, the formation and the decay of excited nuclei, created in nucleus-nucleus collisions at intermediate bombarding energies (10 MeV/u $<$ E $<$ 100 MeV/u) can be investigated. In this energy regime, it is now well known that the collisions are dominated by binary dissipative processes. In such reactions a quasi-projectile and a quasi-target are formed and their excitation energy increases with decreasing the impact parameter. At variance with the phenomenology of deep inelastic reactions at lower energy ($\approx$ 10 MeV/u) an intermediate rapidity region between the quasi-projectile and the quasi-target has been observed which is populated by particles and light fragments [1], [2] (see the contributions of D. Cussol and D. Doré). The size of this zone increases with energy dissipation, becoming predominant for the most central collisions. The physical origin of this mid-rapidity emission is most probably a complicated and highly non-equilibrated interplay between one-body and two-body dissipation. So the detected events have been analyzed globally in order to be independent of the origin of the mid-rapidity emission. The understanding of such reaction mechanisms, in which dynamical effects are predominant, from the beginning of the collision to the secondary decay of the hot primary fragments demands careful analysis with a choice of adequate variables. From this study, we expect to extract valuable information about the global transport properties of nucleons and the different ingredients of the nuclear interaction at zero temperature. Indeed, the nucleons emitted at mid-rapidity should give information about the first steps of the collision. In this context, a comparison with a microscopic transport model is very interesting.
In this contribution, we shall present a comparison between data measured by INDRA for the $^{36}Ar + ^{58}Ni$ system at 95 MeV/u and the prediction of BNV calculations (Boltzman-Nordheim-Vlasov) [3]. We will first discuss the method to be employed and the variables chosen for centrality selection and analysis. In the second part, the results about energy dissipation, charge and isospin transfer, EOS and transport parameters will be presented.

2 General comparison protocol.

The 4π detector INDRA was used to study the $^{36}Ar + ^{58}Ni$ reaction at 95 MeV/u. A description of INDRA can be found in references [4], [5], [6]. In order to keep a maximum of information, we have chosen to consider only quasi-complete events, in which more than 80% of both total charge ($Z_{tot} = 46$) and total incident momentum of the system have been measured.

Concerning the transport model, BNV is a numerical simulation of the nuclear Boltzmann transport equation. In this approach one calculates the space-time evolution of the one-body distribution function under the influence of the the mean field, the nucleon-nucleon collisions and the Pauli principle. For more information about the model and the method employed for computer simulation, see reference [3]. The one-body distribution function gives information about the average properties of the col-

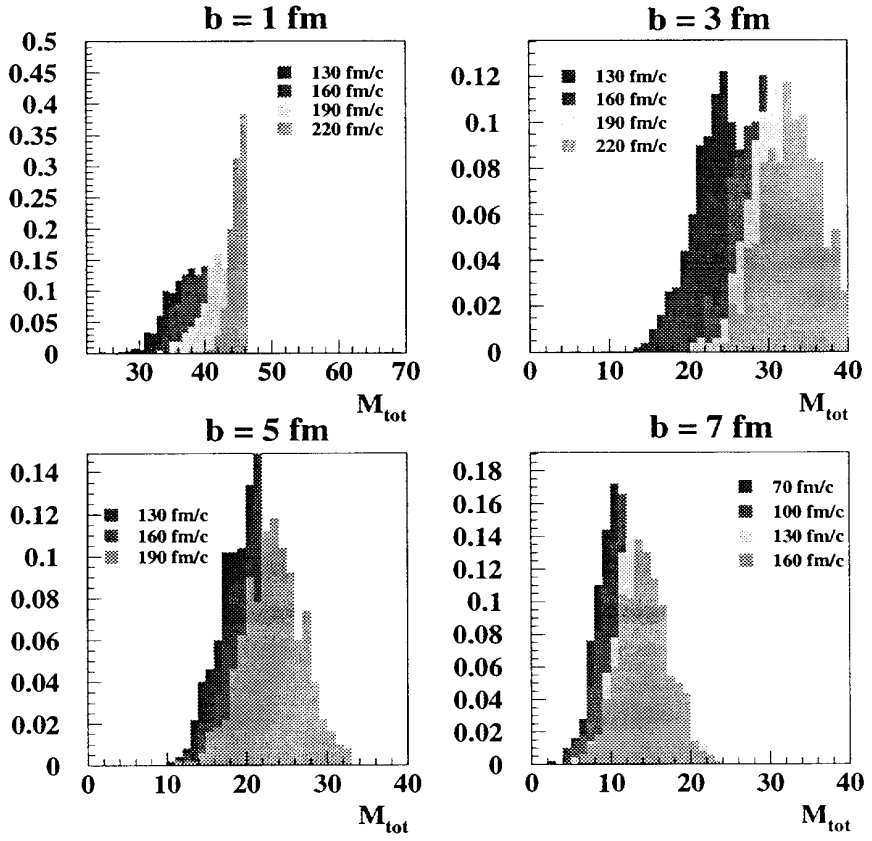

Figure 1: *Charged particle multiplicity distributions for different times T_{clus} and different impact parameters.*

liding nuclear system. BNV can describe thermodynamical variables like pressure, density, temperature, entropy..., as well as collective variables like flow,viscosity, transport coefficients and so on. In this sense BNV can help us to understand the interplay between dynamical and thermodynamical effects in nucleus-nucleus collisions.
For this comparison we have used a Skyrme interaction defined as:

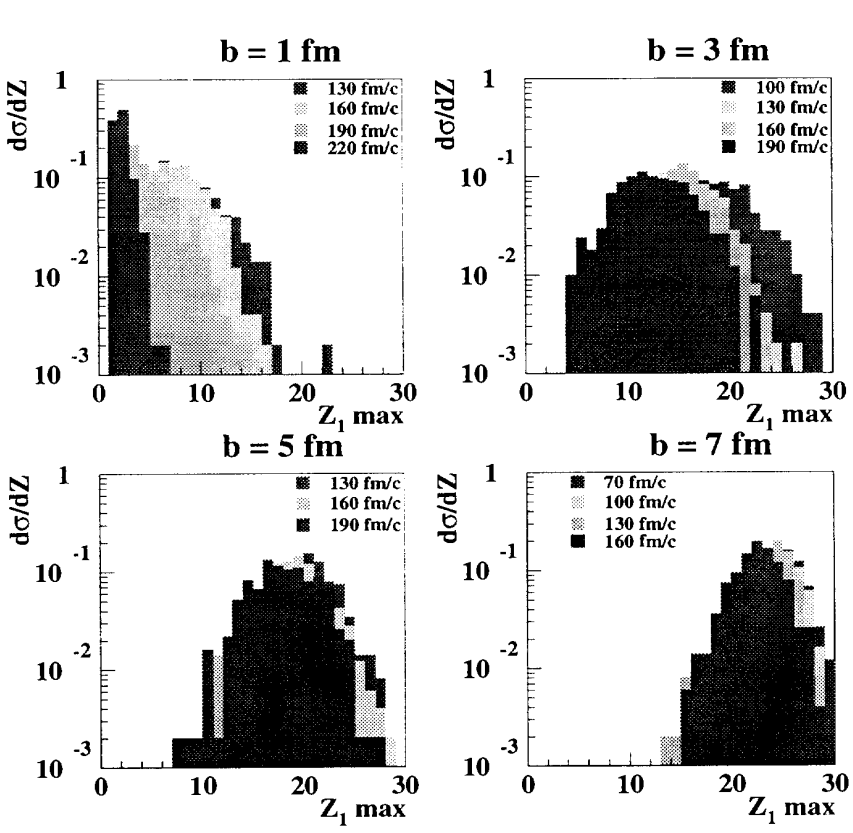

Figure 2: *Heaviest fragment charge distributions for different time T_{clus} and different impact parameters.*

- $U_{MF}(\rho_n, \rho_z) = A\rho + B\rho^\sigma + C\nabla^2\rho + D(\rho_n - \rho_z)\tau_z + U_{coul}(\rho_z)$

where the coefficients C, D are fixed to reproduce the surface and the symmetry terms of the liquid drop energy and A, B are fixed to the saturation point of nuclear matter requiring an incompressibility coefficient $K = 220MeV$. The nucleon-nucleon elastic cross section entering the collision integral was chosen to be the free one

$\sigma_{n-n}(E, \theta, \tau_z)$ where the dependence on energy, scattering angle and isospin is taken from experimental nucleon-nucleon data. With these ingredients, for all impact parameters BNV predicts qualitatively a binary process for the $^{36}Ar + ^{58}Ni$ reaction in the sense that even at b=0 fm, some memory of the entrance channel is kept. But for intermediate impact parameters an important contribution of matter emitted between the projectile and the target is present. And these nucleons are preferentially produced at mid-rapidity.

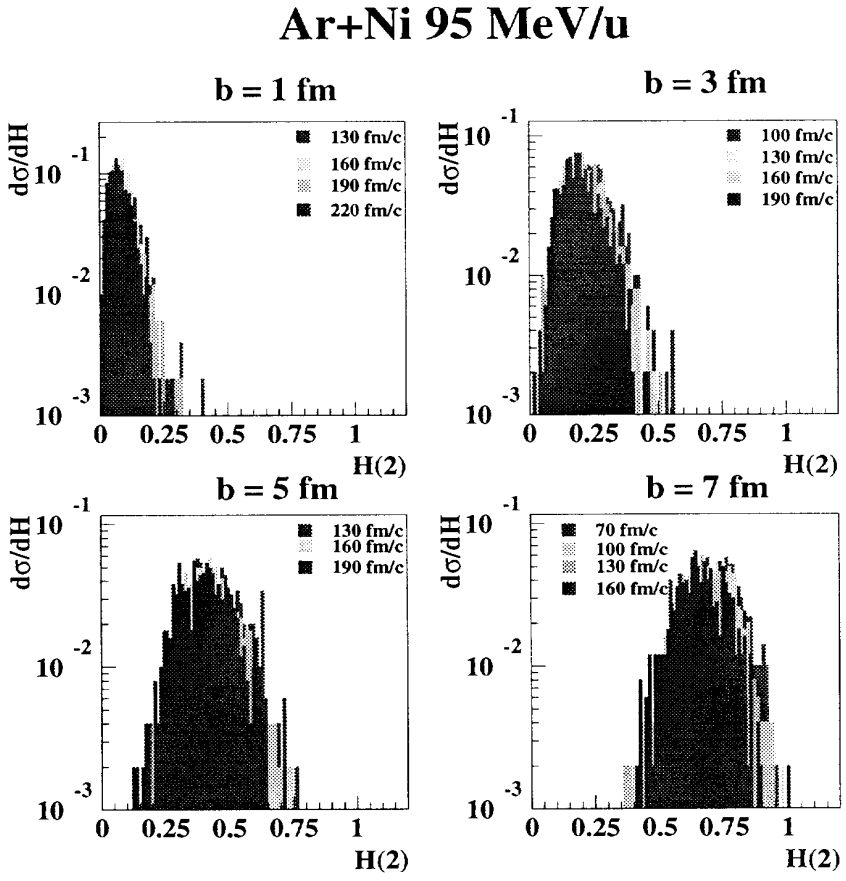

Figure 3: *Second moment of Fox and Wolfram distribution for different times T_{clus} and different impact parameters.*

2.1 Comparison method.

The first question one can ask is : how to compare experimental data and BNV results? Indeed data concern the physical and measurable characteristics of the fragments

(Z, E_{kin}, θ), which are all N-body variables. On the contrary, in the BNV model, one calculates the distribution function, which is a one-body variable.
Two solutions can be proposed. The first one, frequently employed in the literature, consists in calculating N-body variables in the theory. For this purpose, the calculation has to be stopped at the freeze-out time when the dynamics is over. At this time the fragments are formed and their decay can be taken into account by coupling the calculation to an evaporation or multifragmentation code. To be valid this method needs a clearly defined freeze-out time, in the sense that the dynamical and thermodynamical time scales have to be well separated. As we have already mentioned in the introduction, this does not seem to be the case in the collisions we are focusing on, where mid-rapidity emission contaminates the spectators and the important energy dissipation implies comparable time scales for dynamical emission and particle evaporation. Therefore we have chosen to avoid all definition of sources and rather construct

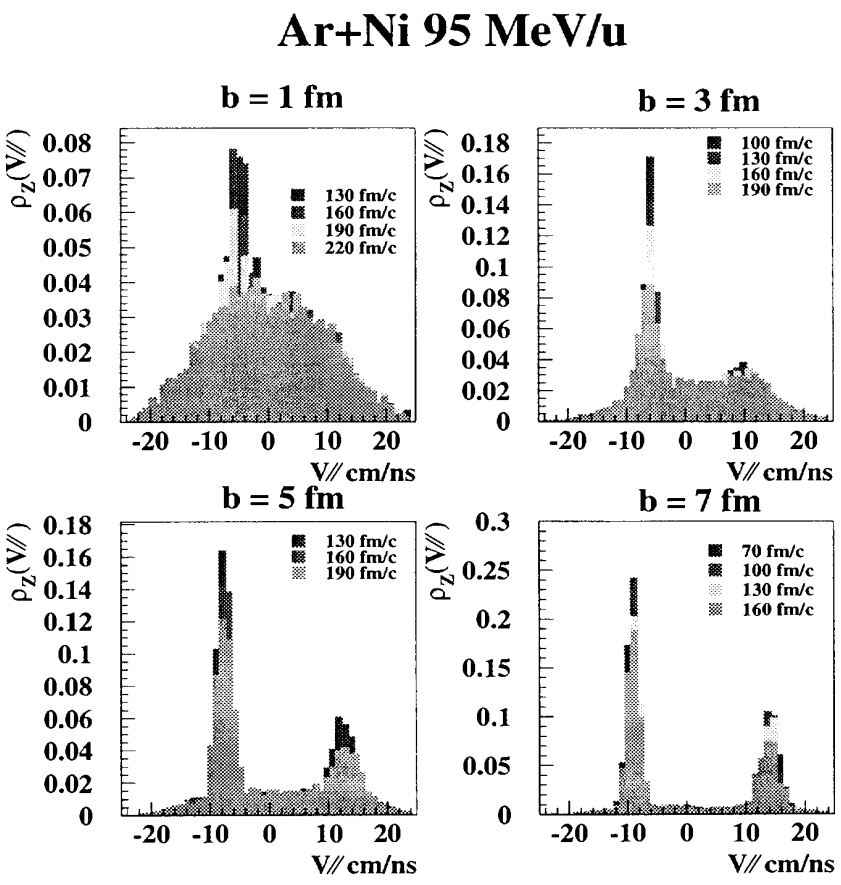

Figure 4: *Charge density for different times T_{clus} and different impact parameters. The parallel velocity is a normalized axis in the ellipsoid frame.*

one-body observables with data. These observables called global variables condensate the experimental information and allow a more simple characterization of the events by a shape description. In this way, the calculation can proceed up to an asymptotic time T_{clus} where nuclear dynamics and secondary evaporation are over. However, even for this maximum time T_{clus} the long range Coulomb correlations are not completely accounted for. Therefore at $t = T_{clus}$ fragments are formed with a coalescence model and Coulomb correlations are added up to infinity. At the end of the calculation, we obtain simulated events which in principle could be treated as experimental events. But one has to stress that the clusterization procedure is here just a trick to subtract Fermi motion from the asymptotic one-body distribution function and completely account for Coulomb correlations. Therefore the variables chosen for the comparison should be independent of the clusterization time T_{clus}.

2.2 Analysis variables

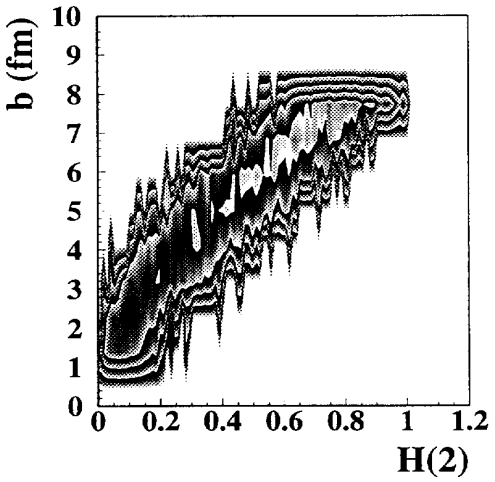

Figure 5: *Correlation between $H(2)$ and the impact parameter.*

In figures 1 and 2 are represented the predicted charged particle multiplicity and heaviest fragment charge distributions for different times T_{clus} and impact parameters. One can see that by increasing T_{clus}, the average multiplicity increases and the charge of the heaviest fragment decreases. Two reasons can be invoked to explain this behavior. The first one is physical. Indeed, when T_{clus} increases the hot fragments evaporate light particles, it is clear that the smaller times shown in the figures cannot yet be considered as aymptotic . The second reason is inherent to BNV. Since the mean field can not describe small fragments the system will vaporize in free nucleons as time goes on. For example, for the most central collisions BNV predicts an unphysical complete vaporization of the system (average multiplicity equal to the total charge of the system

and maximum charge equal to one). In conclusion it is clear that we cannot use for our comparison neither the multiplicity distribution nor the charge of the heaviest residue (except for peripheral collisions).

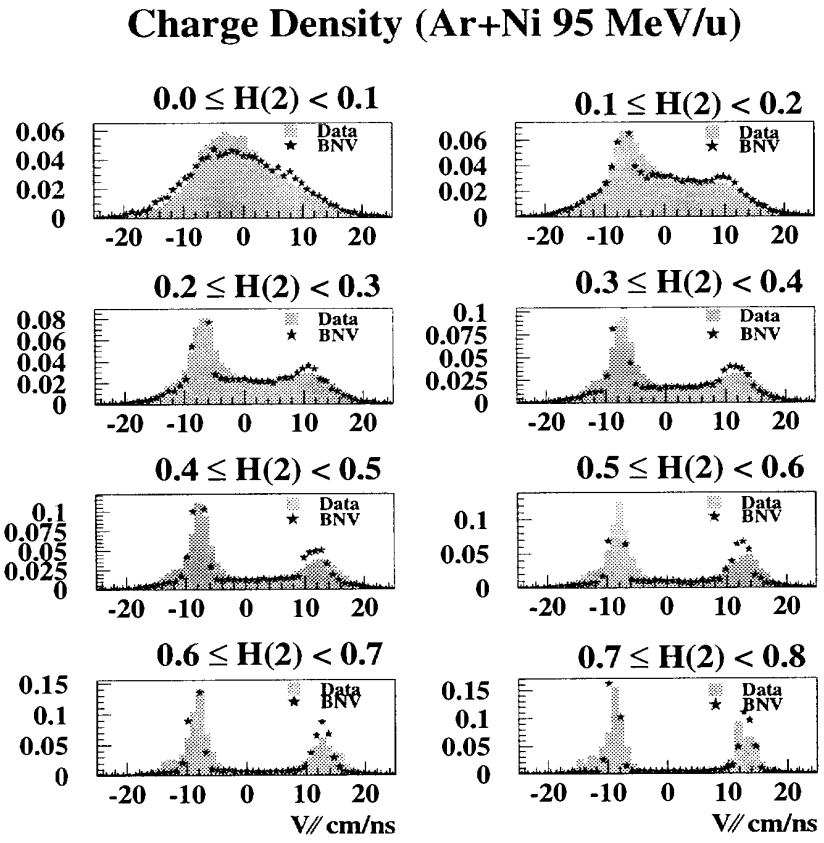

Figure 6: *Comparison between data and BNV for charge density and different bins of* $H(2)$. *The parallel velocity is a normalized axis in the ellipsoid frame.*

Figures 3 and 4 show two examples of global variables, which are independent of T_{clus}. $H(2)$ is the second moment of the Fox and Wolfram distribution [7](figure 3). This variable describes the global shape of the event. For example, $H(2)$ is equal to zero for a spherical event and $H(2)$ is equal to one for a pencil event. The $H(2)$ distribution shows only a very slight dependence on T_{clus}.
The charge density $\rho_z(k)$ (figure 4) is another global variable which represents the shape of the system [8]. It corresponds to the quantity of charge projected on the main axis of the ellipsoid frame. For an intermediate impact parameter, the quasi-projectile and the quasi-target are well separated, but we never have a purely binary process.

An important contribution of matter between the quasi-projectile and the quasi-target can be observed. For all T_{clus}, these three regions do not change, except for the evaporation of the quasi-target mentioned above. But the relative velocity between the quasi-projectile and the quasi-target remains the same as well as the charge density at mid-rapidity. The same independence on T_{clus} is observed on other global variables.

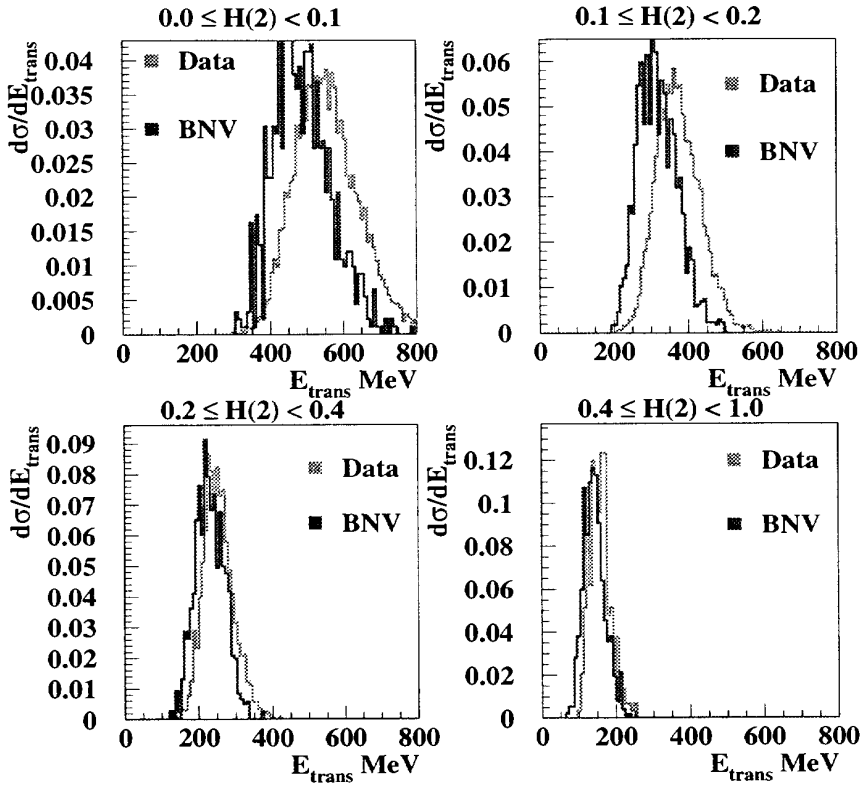

Figure 7: *Comparison between data and BNV for transverse energy and different bins of* $H(2)$.

2.3 Centrality selection.

The comparison cannot be made directly between the inclusive data and the total prediction of BNV by summing up all impact paramaters. In fact due to the finite detection efficiency and completeness requirements of data selection, the experimental impact parameter distribution is deformed. As the experimental impact parameter

values and their distribution are not attainable by direct measurement, we have to find a (global) variable to select centrality both in the theory and in the data.
The violence of the collision can be measured by several global variables. In order to make a suitable choice, we have studied the behaviour of global variables like transverse energy, isotropy ratio, flow angle, $H(2)$... All these variables have a good correlation with the impact parameter, but $H(2)$ is remarkably linear and exhibits a smaller variance than the other ones, this correlation can be seen in figure 5. Therefore the comparison between data and BNV predictions was made with bins of $H(2)$.

3 Results

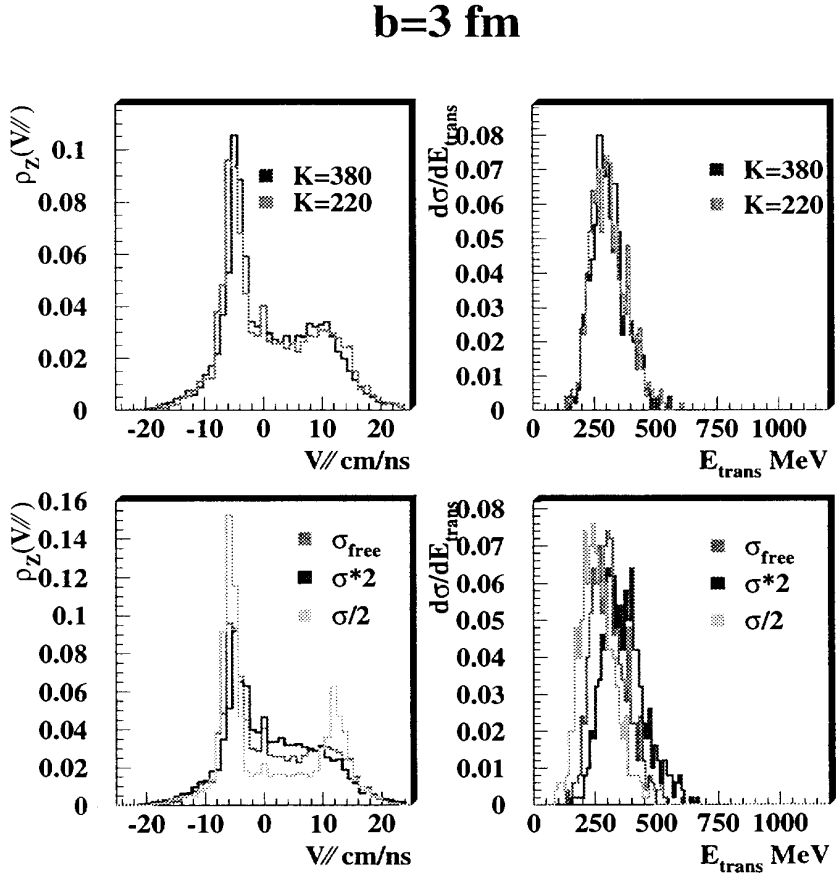

Figure 8: *Behaviour of charge density $\rho_z(k)$ and transverse energy at $b = 3fm$ for different values of K and σ_{n-n}. For charge density the velocity axis is the same than in figure 4.*

The results of our analysis for the charge density $\rho_z(k)$ are represented in figure 6. The relative position between the quasi-projectile peak and the quasi-target peak is well reproduced as well as the population at mid-rapidity. These results indicate that the dissipation is well described in BNV. We have checked that the quality of the agreement is not due to an autocorrelation between the selection variable $H(2)$ and the analysis variable $\rho_z(k)$. In fact, very similar results are obtained if the charge density is analyzed in bins of other global variables uncorrelated to the parallel velocity axis like transverse energy. A complementary piece of information is given by the transverse energy which is correlated with the perpendicular axis of the reaction frame. The results are shown in figure 7.

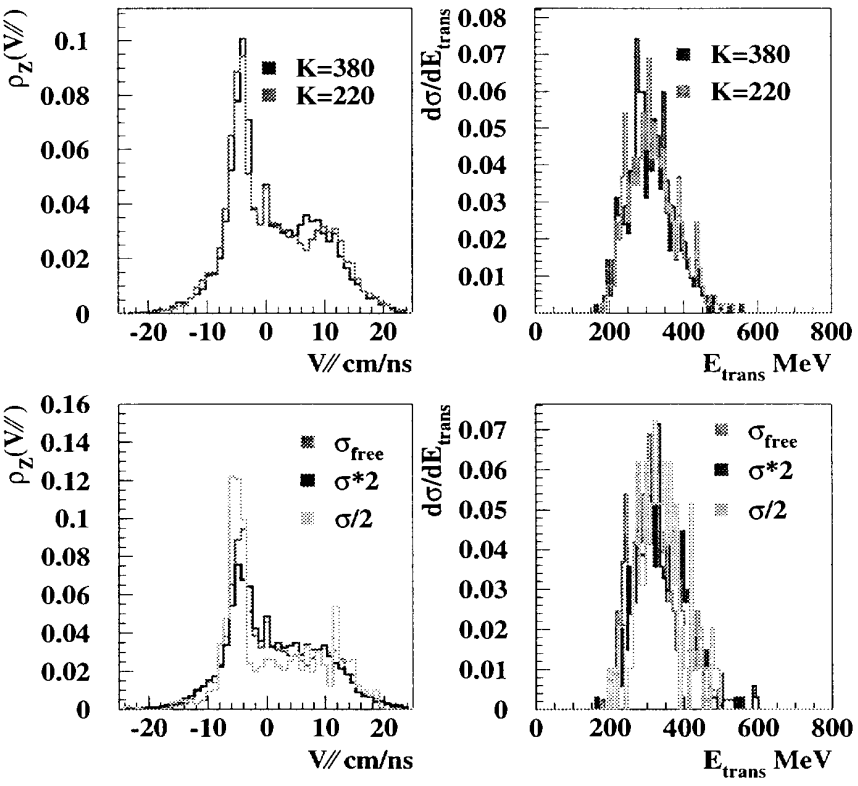

Figure 9: *Behaviour of charge density $\rho_z(k)$ and transverse energy for $0.2 \leq H(2) \leq 0.3$ when K and σ_{n-n} change. For charge density the velocity axis is the same than in figure 4.*

For the most peripheral collisions, BNV well reproduces the data. We can see a disagreement in central collisions where the transverse energy is systematically underes-

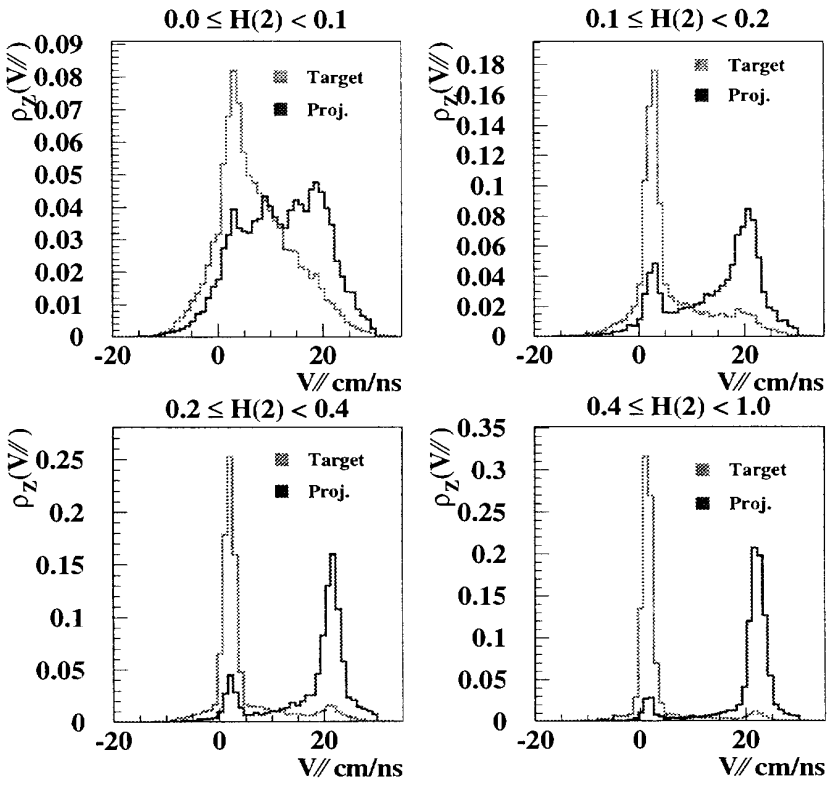

Figure 10: *Origin of nucleons at the beginning of a reaction. The parallel velocity axis is a normalized axis in the laboratory frame.*

timated by about 20 %. In order to understand the physical origin of this discrepancy we have studied the sensitivity of global observables to the parameters of the interaction used in the model. We have changed the incompressibility coefficient K and the nucleon-nucleon cross section σ_{n-n}. Some results are represented in figure 8, for $K = 380$ MeV and $K = 220$ MeV, which is the one used above and for three different values of σ_{n-n}: $\sigma_{n-n} = \sigma_{free}$ (the one used above), $\sigma_{n-n} = 2 * \sigma_{free}, \sigma_{n-n} = \sigma_{free}/2$. Compressibility does not influence much the mid-rapidity region, but for the highest K value, the quasi-projectile and the quasi-target peaks are slightly closer. This trend is systematically observed for all impact parameters, consequently it seems that $K = 220$ MeV better reproduces the data. But a variation of K does not change the behaviour of transverse energy.

The effects of a variation of σ_{n-n}, on these two variables are much more pronounced. Indeed, the higher is the cross section employed the larger is the contribution to mid-

rapidity and the lower is the transparency. The relative velocity between the quasi-projectile and the quasi-target peaks are smaller. As expected the transverse energy increases with σ_{n-n}. But the behaviour of these two global variables is not the same once they are analyzed in $H(2)$ bins. Centrality is defined by the shape of events which itself depends on the parameters of the interaction. Therefore globally the differences due to the variation of the parameters are much less visible than with an impact parameter selection, as we can see in figure 9.
A small effect can still be seen for the charge density $\rho_z(k)$, in particular at mid-rapidity. In summary, the best set of parameters seems to be a soft equation of state and the free nucleon-nucleon cross section.

In order to extract information on transport properties of nuclear matter it is essential to well understand all the terms of the nuclear interaction. The global transport properties of the nucleons can be investigated through several parameters like mass transfer and isospin transfer. For the mass transfer study, we have calculated the charge density $\rho_z(k)$ for different centrality bins, selected with $H(2)$, showing separately the nucleons which originally belonged to the projectile and to the target (figure 10).
This picture shows that the charge exchange goes preferentially from the projectile to the target and the mid-rapidity region is more populated by the projectile nucleons than by the target nucleons.

An interesting part of the interaction is the symmetry energy, which is correlated with isospin transfer. With the same philosophy as before an "isospin density" was built. In theoretical predictions, we calculate for free nucleons the ratio of neutron and proton numbers in each velocity bin and for each bin of $H(2)$. For experimental data, as we have no neutron measurement, we calculate the ratio of tritons over ^3He in each velocity bin and for the same bins of $H(2)$. The results are shown in figure 11.
In the data the mid-rapidity zone is neutron rich and the quasi-projectile region is proton rich. On the contrary, the theoretical ratio is constant and equal to one, which is the initial isospin ratio of the system. The density dependence of the symmetry term of the Skyrme interaction used for this calculation was very schematic. So this behaviour about the inhomogeneity of the isospin density might bring information about the symmetry energy.

4 Conclusions

In this contribution, we have shown that a meaningful comparison between experimental data and a one-body transport model as BNV is possible by means of an extensive use of global variables. The same technique of analysis can be employed for this model and the data and no artificial cut has to be introduced in order to define nuclear sources. The comparison gives a good overall reproduction of data by assuming a soft equation of state and no important modifications of the free the nucleon nucleon cross section.

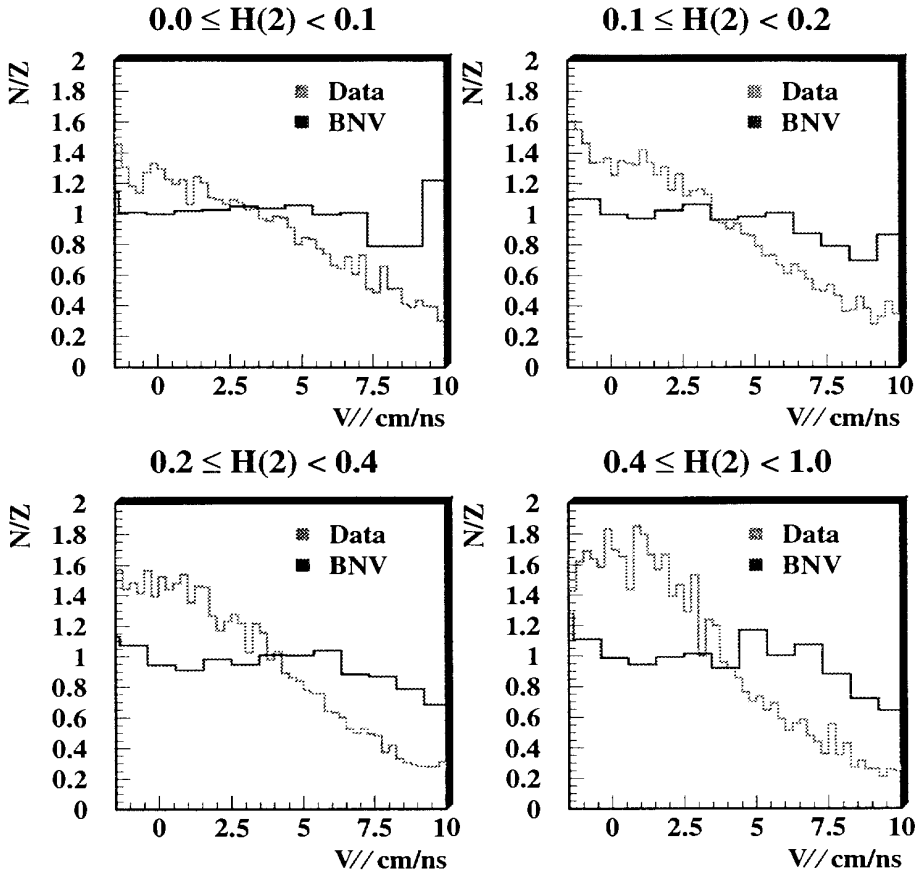

Figure 11: *Isospin versus velocity: comparison between data and BNV predictions for several $H(2)$ bins. The parallel velocity axis is calculated in the center of mass frame.*

However a 20 % underestimation of the transverse energy for the most central collisions is observed which requires further studies. The mid-rapidity zone is neutron rich and it could be related to the density dependence of symmetry energy in the equation of state. For a better understanding of this point we plan to replace the interaction which is presently in BNV with a recently proposed Skyrme interaction involving an isospin dependence optimized to exotic nuclei and neutron matter [9].

References

[1] J. Lukasik et al. *Phys. Rev.* C55 (1997) 1906.

[2] T. Lefort. PhD thesis, Université de Caen, 1997.

[3] A. Bonasera et al. *Phys. Rep.* 243 (1994) 1.

[4] J. Pouthas et al. *Nucl. Inst. and Meth.* A357 (1995) 418.

[5] J-C. Steckmeyer et al. *Nucl. Inst. and Meth.* A361 (1995) 472.

[6] J. Pouthas et al. *Nucl. Inst. and Meth.* A369 (1995) 222.

[7] G.C. Fox and S. Wolfram. *Nucl. Phys.* B419 (1979) 413.

[8] J-F. Lecolley. Internal Report LPC, June 29,1996.

[9] E. Chabanat et al. *Nucl. Phys.* A627 (1997) 710.